Crystallization and Melting Behavior of *trans*-1,2-Syndiotactic Polypentadiene

Fabio Bertini, Maurizio Canetti, Giovanni Ricci

Istituto per lo Studio delle Macromolecole–C.N.R., Via E. Bassini 15-20133 Milano, Italy

Received 30 July 2004; accepted 14 January 2005
DOI 10.1002/app.22022
Published online in Wiley InterScience (www.interscience.wiley.com).

ABSTRACT: (E)-1,3-pentadiene was polymerized at −30°C by using the catalyst system $CoCl_2(P^iPrPh_2)^2$–MAO. A *trans*-1,2-syndiotactic structure was attributed to the semicrystalline polymer obtained on the basis of the characterization carried out by FTIR, NMR, and WAXD techniques. The thermal behavior of the polypentadiene was investigated by thermogravimetry and differential scanning calorimetry. Isothermal melt crystallization kinetics were analyzed according to the Avrami equation. Nonisothermal crystallization kinetics were elaborated by using Ziabicki and Avrami methods modified by Jeziorny. The equilibrium melting temperature was calculated. The thermal behavior of *trans*-1,2-syndiotactic polypentadiene was compared with that of 1,2-syndiotactic polybutadiene. © 2005 Wiley Periodicals, Inc. J Appl Polym Sci 97: 1970–1976, 2005

Key words: differential scanning calorimetry (DSC); thermal properties; crystallization; melting point; kinetics

INTRODUCTION

In the last few years, the study of the synthesis and the properties of 1,3-dienes homo- and copolymers has received a renewed impulse, due to the introduction of more active and stereospecific catalysts based on methylaluminoxane. Several stereoregular polymers having different microstructures (*cis*-1,4; *trans*-1,4; 1,2; 3,4) and tacticity (iso- and syndiotactic) were obtained from different conjugated dienes.[1–4]

Recently, we reported on the synthesis and characterization of $CoCl_2(P^iPrPh_2)_2$ and its use, associated to methylaluminoxane, in the polymerization of various 1,3-dienes [butadiene, (E)-1,3-pentadiene, 1,3-hexadiene, 3-methyl-1,3-pentadiene]. This catalyst was found to be extremely active and stereospecific, giving essentially 1,2-semicrystalline polymers from the above reported monomers.[5]

In our previous works, we detailed investigations on the thermal behavior of 1,2-syndiotactic polybutadiene and butadiene-isoprene copolymers obtained by using $CrCl_2(dmpe)_2$–methylaluminoxane (MAO) as catalyst system.[6–7]

In the present article, we report structural characteristics and thermal properties of *trans*-1,2-syndiotactic polypentadiene (*trans*-1,2-PPD) obtained with the system $CoCl_2(P^iPrPh_2)_2$ at −30°C.[8] In particular, this article reports on the melting behavior and the isothermal and nonisothermal crystallization kinetics of *trans*-1,2-PPD.

Correspondence to: F. Bertini (bertini@ismac.cnr.it).

Journal of Applied Polymer Science, Vol. 97, 1970–1976 (2005)

EXPERIMENTAL

Polymer synthesis

Heptane (14.2 mL, >99.8% pure, Baker, Phillipsburg, NJ), (E)-1,3-pentadiene (4 mL, 99% pure, Aldrich, Milwaukee, WI), and MAO (1×10^{-3} mol; 0.63 mL, 10% wt% toluene solution, Crompton, Middlebury, CT) were introduced in a 50-mL dried flask. The solution so obtained was cooled at −30°C and then $CoCl_2(P^iPrPh_2)_2$ (1×10^{-5} mol, 3 mL of a 2 mg/mL toluene solution) was added. All operations were carried out under dry nitrogen. The polymerization was terminated by adding methanol containing a small amount of hydrochloric acid after 1 month. The polymer was coagulated and repeatedly washed with fresh methanol and then dried in vacuum at room temperature. Polymer yield was 1.87 g.

Polymer structural characterization

Fourier transform infrared (FTIR) spectrum was recorded with a Bruker Tensor 27 spectrometer by using sample in KBr pellets.

^{13}C- and ^{1}H-NMR measurements were performed on Bruker AM 270 and Avance 400 instruments. The spectra were obtained in $C_2D_2Cl_4$ at 103°C by using hexamethyldisiloxane as internal standard. The concentration of the polymer solutions was about 10 wt %.

The wide-angle X-ray diffraction (WAXD) data were obtained at 20°C by using a Siemens D-500 dif-

fractometer equipped with a Siemens FK 60-10 2000-W tube (CuK_α radiation, $\lambda = 0.154$ nm). The operating voltage and current were 40 kV and 40 mA, respectively. The data were collected from 5 to 40 $2\theta°$ at 0.02 $2\theta°$ intervals.

Thermal characterization

Thermogravimetry (TG) analyses were carried out with a Perkin–Elmer TGA 7 instrument. The samples (~ 5 mg) were heated at 10°C min^{-1} under a nitrogen atmosphere (60 mL min^{-1}). TG and derivative thermogravimetry (DTG) curves were recorded from 50 to 600°C.

The isothermal and nonisothermal crystallization kinetics and the melting behavior of syndiotactic *trans*-1,2-PPD were investigated by differential scanning calorimetry (DSC) by using a Perkin–Elmer Pyris 1 system equipped with a liquid subambient device. The instrument was calibrated with indium standard. The sample weight was 2.5–3 mg and a fresh specimen was used for each run.

In a typical isothermal crystallization run, the polymer was heated up to 200°C and held at this temperature for 3 min to cancel previous thermal history. Then, the sample was cooled at a nominal rate of 500°C min^{-1} to the selected crystallization temperature (T_c). The heat flow evolved during the isothermal crystallization was recorded as a function of time. Finally, the isothermally crystallized sample was heated with a scan rate of 10°C min^{-1} from T_c to 200°C, determining the melting temperature (T_m).

The following standard procedure was employed in nonisothermal crystallization analysis: the samples were heated up to 200°C and kept for 3 min and then cooled at various cooling rates ranging from 2 to 40°C min^{-1}. The exothermic crystallization peak was recorded as a function of temperature.

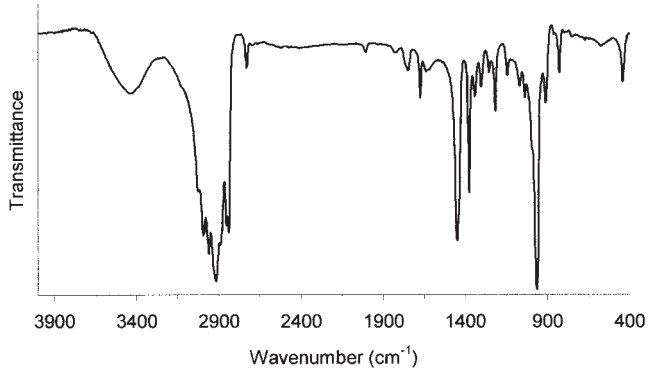

Figure 1 FTIR spectrum of *trans*-1,2-PPD.

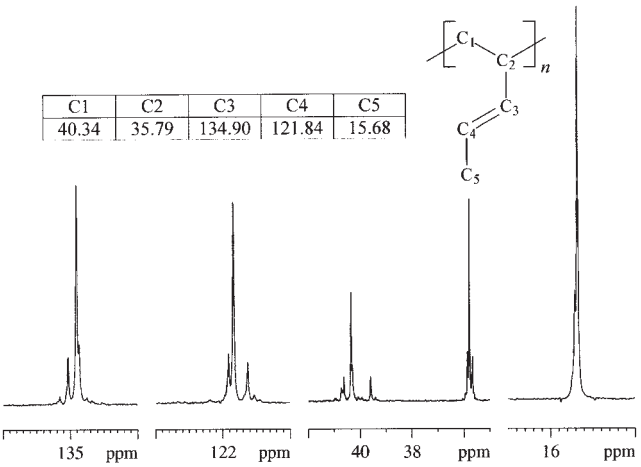

Figure 2 ^{13}C-NMR spectrum of *trans*-1,2-PPD.

RESULTS AND DISCUSSION

Polymer structural characterization

The catalyst system $CoCl_2(P^iPrPh_2)_2$ polymerizes (E)-1,3-pentadiene to semicrystalline *trans*-1,2-syndiotactic polymer. The FTIR spectrum of *trans*-1,2-PPD, reported in Figure 1, is characterized by two typical absorptions: the intense band at 963 cm^{-1} assigned to the out-of-plane vibration of hydrogen atoms adjacent to the double bond and the band at 1376 cm^{-1} due to the methyl group of 1,2-pentadiene units.[9–10]

The ^{13}C-NMR spectrum of the polymer, assigned as already reported in our previous article,[8] is shown in Figure 2 and is consistent with a *trans*-1,2-syndiotactic structure (1,2 content ~ 99%; percentage of syndiotactic pentads, [rrrr] %, ~ 60%). The syndiotacticity of the polymer is also indicated by the ^{1}H-NMR spectrum (Fig. 3); in fact, it can be observed that the resonance of

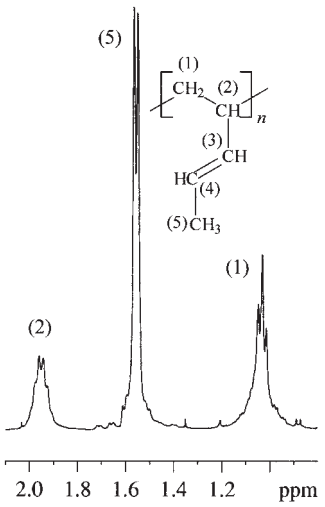

Figure 3 ^{1}H-NMR spectrum of *trans*-1,2-PPD.

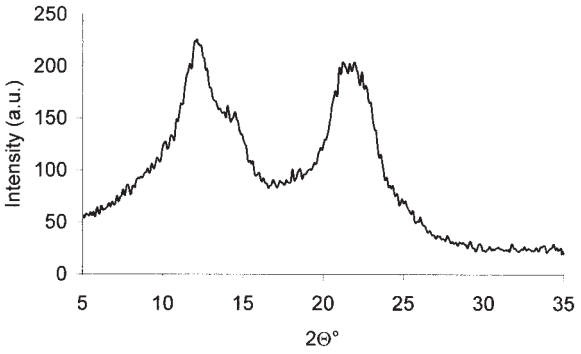

Figure 4 X-ray powder spectrum of *trans*-1,2-PPD.

the methylene protons at 1.02 ppm is a triplet, as expected for a syndiotactic polymer.[11]

The WAXD profile of the synthesized *trans*-1,2-PPD is reported in Figure 4. The position at maximum intensity of the diffraction angles, 2θ, for the two higher registered peaks, correspond to the spacings of 0.73 and 0.41 nm, respectively. The presence of a shoulder following the first peak was evidenced at 0.62 nm.

Thermal characterization

Thermogravimetry

The TG and DTG thermograms of *trans*-1,2-PPD are reported in Figure 5. On heating at 10°C/min, the polymer volatilizes completely in a single step. The chain fragmentation with the formation of volatile

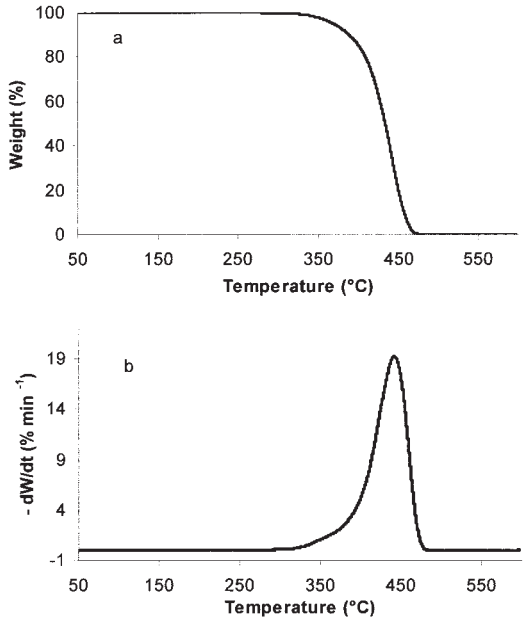

Figure 5 Thermogravimetric (a) and derivative thermogravimetric (b) curves of *trans*-1,2-PPD in nitrogen at 10°C min^{-1}.

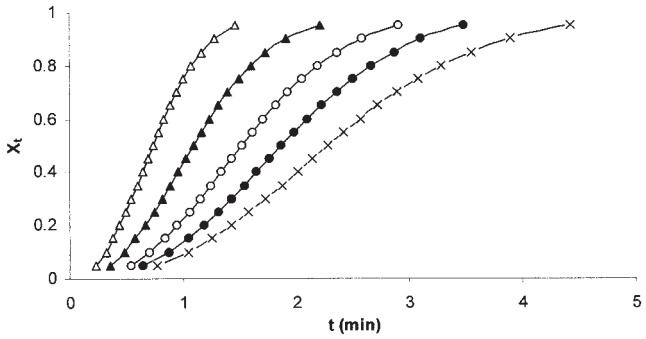

Figure 6 Development of relative crystallinity with time for isothermal melt crystallization at the adopted T_c (°C): 150 (×), 148 (●), 146 (○), 144 (▲), 142 (△).

products occurs only at temperatures higher than 300°C. In fact, the weight loss calculated at 300°C is ~ 1%. The maximum rate of degradation takes place at 442°C and the decomposition is complete at ~ 500°C.

Isothermal crystallization kinetics

The crystallization process, determined by DSC, is very marked by temperature dependence. Isothermal crystallizations were performed at 142, 144, 146, 148, and 150°C. Figure 6 reports the mass fraction of polymer crystallized from melt at time t, X_t, as functions of crystallization time at five different crystallization temperatures. In Table I, the half-time of crystallization $t_{0.5}$, defined as the time at which the extent of crystallization is completed 50%, is reported for different T_c. The reciprocal of $t_{0.5}$, $\tau_{1/2}$, can be used as the crystallization rate at 50% crystallinity:

$$\tau_{0.5} = 1/t_{0.5} \quad (1)$$

The $\tau_{0.5}$ values are summarized in Table I. When increasing T_c, the crystallization exotherm peak shifted to longer times; it implies that $t_{0.5}$ increases (i.e., the rate of crystallization decreases).

TABLE I
Isothermal Crystallization Kinetics Parameters of *trans*-1,2-PPD

T_c(°C)	t_{max} (min)[a]	n	K_n (min^{-n})	$t_{0.5}$ (min)	$\tau_{0.5}$ (min^{-1})
142	0.783	2.23	1.3583	0.736	1.359
144	1.133	2.23	0.5563	1.095	0.913
146	1.467	2.41	0.2464	1.517	0.659
148	1.800	2.43	0.1494	1.870	0.535
150	2.283	2.35	0.0973	2.281	0.438

[a] Peak time of the crystallization exotherm.

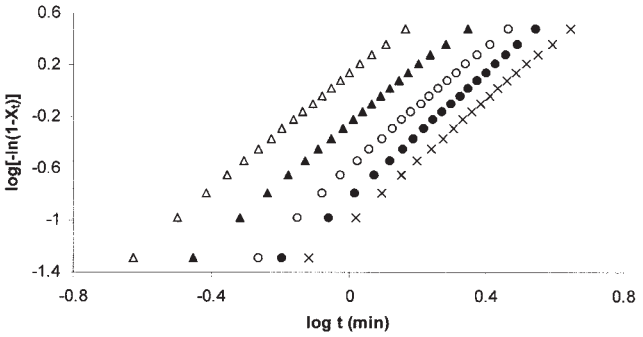

Figure 7 Avrami plots of $\log[-\ln(1 - X_t)]$ versus $\log t$ for isothermal melt crystallization of *trans*-1,2-PPD at the adopted T_c (°C): 150 (×), 148 (●), 146 (○), 144 (▲), 142 (△).

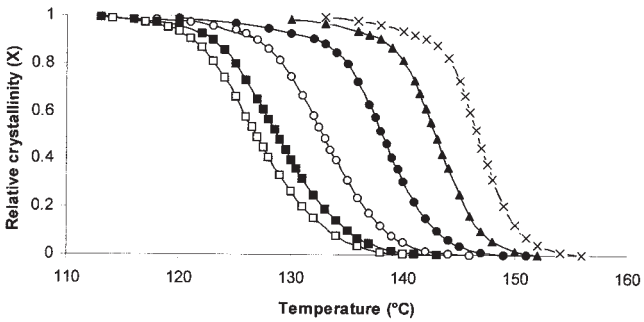

Figure 9 Relative crystallinity versus temperature for nonisothermal crystallization of *trans*-1,2-PPD at the adopted cooling rates (°C min^{-1}): 40 (□), 30 (■), 20 (○), 10 (●), 5 (▲), 2 (×).

The isothermal crystallization kinetics of the *trans*-1,2-PPD was interpreted in terms of the Avrami equation[12–13]

$$1 - X_t = exp(-K_n t^n) \tag{2}$$

where K_n is an overall crystallization rate constant including contributions from crystal growth and nucleation, and n is an exponent that contains contributions related to the crystal growth geometry and the time dependency of the nucleation rate. Table I collects the values of n and K_n determined from the slope and the intercept, respectively, of the straight lines obtained by plotting $\log[-\ln(1 - X_t)]$ versus $\log t$.

In Figure 7, the Avrami plots, obtained at different isothermal crystallization temperatures for PP, are reported. For all T_c investigated, a straight line with a good correlation was generally observed for X_t values included between 0.05 and 0.95. A fractional value of the Avrami exponent, n, ranging from 2.2 to 2.4, was observed for the adopted crystallization temperatures. The crystallization rate parameter K_n decreases with the increased T_c.

The value of the activation energy for the crystallization process was calculated assuming that the crystallization rate parameter K_n can be approximately described by an Arrhenius form[14]

$$K_n^{1/n} = K_0 exp(-\Delta E/RT) \tag{3}$$

where K_0 is a temperature-independent preexponential factor, R is the universal gas constant, and T is the absolute temperature. ΔE is the total activation energy and consists of the transport activation energy and the nucleation activation energy.[15] The ΔE value of −203 kJ/mol was calculated from the slope of the Arrhenius plot of $(1/n)\ln(K_n)$ versus $1/T_c$ (Fig. 8).

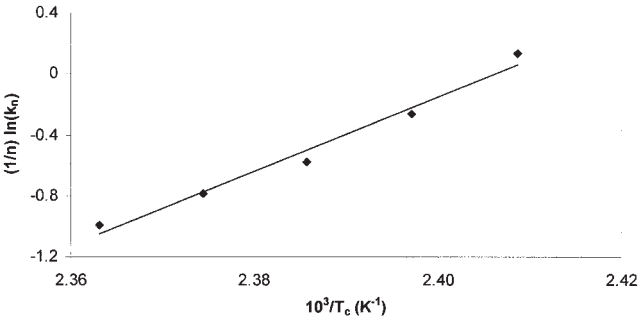

Figure 8 Arrhenius plot of $(1/n)\ln(k_n)$ versus $1/T_c$ for determining the activation energy of crystallization.

Nonisothermal crystallization kinetics

The development of relative crystallization with temperature, determined by DSC, for nonisothermal melt crystallization of *trans*-1,2-PPD at different cooling rates, ranging from 2 to 40°C min^{-1}, is presented in Figure 9.

According to the relationship between time (t) and temperature (T),

$$t_x = (T_i - T_x)/\phi \tag{4}$$

where Φ is the cooling rate, and T_i and T_x are the temperature at the initial time and a time x during the cooling run, respectively; the dependence of relative crystallinity on time can be calculated.

The temperature at the maximum of the exothermic peak (T_{max}) shifted to a lower temperature region as the cooling rate increased. The T_{max} values, the corresponding times (t_{max}), and the crystallization enthalpy (ΔH_c) are reported in Table II.

In a nonisothermal crystallization, the activation energy ΔE can be calculated considering the variation of crystallization peak temperature T_{max}, with the cooling rate Φ, by the Kissinger equation[16]

$$-\Delta E = R[d(ln\phi/T_{max}^2)/d(1/T_{max})] \tag{5}$$

TABLE II
Nonisothermal Crystallization Parameters of *trans*-1,2-PPD

ϕ (°C min^{-1})	T_{max} (K)	t_{max} (min)	ΔH_c (J/g)
2	419.6	2.54	29.4
5	416.0	1.25	31.1
10	411.3	0.72	33.7
20	405.9	0.44	34.3
30	401.5	0.34	33.1
40	399.4	0.27	32.1

where R is the universal gas constant. The ΔE value of -201 kJ/mol was calculated from the slope by plotting $\ln(\Phi/T_{max}^2)$ versus $1/T_{max}$ (Fig. 10). Compared with the isothermal crystallization activation energy calculated above, they exhibit very good agreement.

The crystallization rate coefficient (CRC), defined as the variation in cooling rate required to change the undercooling of the polymer melt by 1°C, was introduced by Khanna.[17] The CRC can be obtained from the slope by plotting the cooling rate versus T_{max} and can be used as a guide for ranking the polymers on a scale of crystallization rates. The CRC values are higher for faster crystallizing systems. A CRC value of 122 h^{-1} was calculated for *trans*-1,2-PPD by using the T_{max} obtained by cooling the sample at five different rates ranging from 5 to 40°C min^{-1}. This value is higher than those reported for polyethylene and polypropylene,[18] but is lower than the one obtained for 1,2-syndiotactic polybutadiene.[6]

As suggested by Jeziorny, the kinetics of nonisothermal crystallization can be characterized by the application of two different procedures.[19] One procedure is based directly on the approximate theory formulated by Ziabicki, in which the crystallization can be presented by means of the equation for first-order kinetics[20–22]

$$dX/dt = [1 - X]K(T) \tag{6}$$

where X is the relative crystallinity, and $K(T)$ is the rate constant dependent only on temperature. A $K(T)$ value can be determined at a temperature T in the range of temperatures between glass transition and melting temperatures.

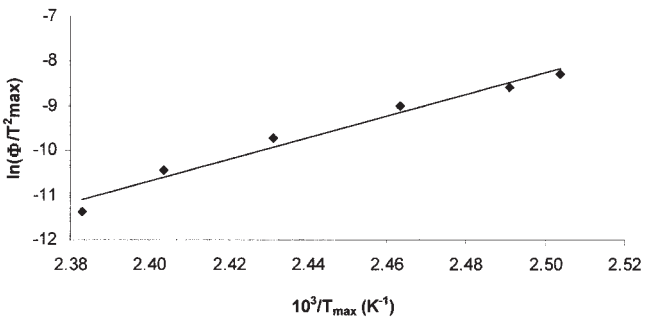

Figure 10 Plot of $\ln(\phi/T_{max}^2)$ versus $1/T_{max}$ according to the Kissinger method.

TABLE III
Nonisothermal Crystallization Kinetic Parameters of *trans*-1,2-PPD

ϕ (°C min^{-1})	D (K)	K_{max} (min^{-1})	G (K min^{-1})	G_c
2	5.608	0.520	3.104	1.552
5	6.673	0.949	6.744	1.349
10	7.574	1.694	13.797	1.380
20	9.687	2.567	26.465	1.323
30	10.612	3.705	41.848	1.395
40	10.694	5.103	58.088	1.452

According to Ziabicki's theory, Jeziorny derived an equation to calculate the quantity G, defined as the kinetic crystallizability, by means of nonisothermal crystallization[19]

$$G = \int_{T_g}^{T_m} K(T)dT = (\pi/ln2)^{1/2}K_{max}D/2 \tag{7}$$

where K_{max} is the value of $K(T)$ at the maximum crystallization rate, and D is the half-width of the crystallization peak. The parameter G must be corrected considering the effect of cooling rate (dT/dt), and its final form is

$$G_c = G/(dT/dt) \tag{8}$$

where G_c means the kinetic crystallizability at unit cooling rate.

Calculation of the G_c parameter was made possible by knowing the D and K_{max} values appearing in eq. (7). The half-width D can be directly determined from the thermogram, and the K_{max} value can be calculated as

$$K_{max} = C_k/t_{max} \tag{9}$$

where

$$C_k = \int_0^{t_{max}} (dH/dt)dt \Big/ \int_{t_{max}}^{\infty} (dH/dt)dt \tag{10}$$

where t_{max} is the time from the start of crystallization to reaching the maximum rate of crystallization.

The calculated parameters characterizing the *trans*-1,2-PPD nonisothermal crystallization, according to Jeziorny approach, are shown in Table III. The G_c values show a quite constant value for all investigated cooling rates (i.e., the kinetic crystallizability is related only to the intrinsic structure of the polymer).

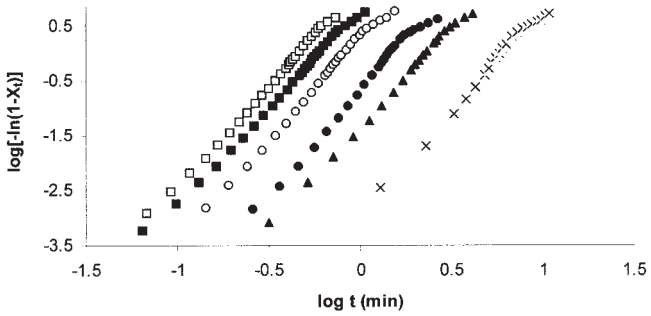

Figure 11 Avrami plots of $\log[-\ln(1 - X_t)]$ versus $\log t$ for nonisothermal melt crystallization of *trans*-1,2-PPD at the adopted cooling rates (°C min^{-1}): 40 (□), 30 (■), 20 (○), 10 (●), 5 (▲), 2 (×).

The second procedure is based on the acceptance of the simplifying assumption that crystallization occurs under constant temperature. In this case, the method to describe the crystallization kinetic is based on the Avrami equation, which assumed that the relative degree of crystallinity developed with crystallization time t[12]

$$1 - X_t = exp(-Z_t t^n) \tag{11}$$

where X_t is the relative degree of crystallinity at time t, Z_t is the rate constant, and n is the Avrami exponent in the nonisothermal crystallization process. It must be taken into account that in nonisothermal crystallization, the Z_t and n parameters do not have the same physical meaning as in the isothermal crystallization.[23] Considering the nonisothermal character of the process investigated, the Z_t value determined must be corrected considering the effect of cooling rate

$$Z_c = Z_t/(dT/dt) \tag{12}$$

The values of n and Z_t were derived from the slope and the intercept, respectively, of the straight lines obtained by plotting $\log[-\ln(1 - X_t)]$ versus $\log t$ (Fig. 11). The data reported in Figure 11 are linear over a wide range of X_t; the deviation from the initial linear trend was observed when the X_t values were around 0.85, and it was considered due to secondary crystallization phenomena.

The results of the Avrami analysis for nonisothermal crystallization are listed in Table IV. The n values observed were low dispersed, ranging from 3.6 to 4.0. As observed for the isothermal crystallization, nonintegral values of the Avrami exponent were obtained.

The Ozawa equation is a modification of the Avrami equation which considers the effect of the cooling rate on crystallization from the melt, replacing the crystallization time in isothermal conditions with the cooling rate Φ[24]

TABLE IV
Nonisothermal Crystallization Kinetic Parameters of *trans*-1,2-PPD Obtained from Avrami Analysis

ϕ (°C min^{-1})	n	$\log Z_t$	Z_c (min^{-n}/°C)
2	3.81	−2.97	0.033
5	3.75	−1.37	0.208
10	3.97	−0.67	0.858
20	3.91	0.34	1.039
30	3.63	0.81	1.064
40	3.63	1.20	1.072

$$1 - X = exp[-K_c(T)/\phi^m] \tag{13}$$

where X is the relative crystallinity at temperature T, K_c(T) is the cooling function of the process, and m is the Ozawa exponent dependent on the crystal growth and nucleation mechanism. The results of the Ozawa analysis are presented in Figure 12 by plotting $\log[-\ln(1 - X)]$ versus $\log \Phi$ for temperatures in the range of 133 to 139°C. The nonlinear trend in Figure 12 means that the parameter m is not a constant during crystallization. As observed for some polymers,[25–29] the crystallization under nonisothermal conditions could not be described by using the Ozawa equation, probably because of the inaccurate assumptions about secondary crystallization and folded length of the polymer chain in Ozawa's theory.

Melting behavior

The observed melting temperature (T_m), determined by DSC, linearly increases with the isothermal crystallization temperature (T_c) for *trans*-1,2-PPD. The experimental data can be fitted by the Hoffman–Weeks equation[30]

$$T_m = (1/\gamma)T_c + (1 - 1/\gamma)T_m^0 \tag{14}$$

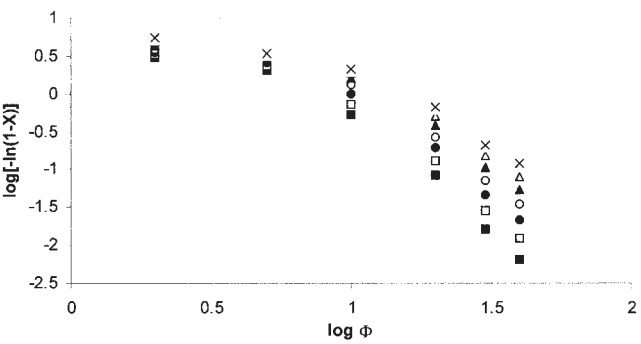

Figure 12 Ozawa plots of $\log[-\ln(1 - X)]$ versus $\log \phi$ for nonisothermal crystallization of *trans*-1,2-PPD at various temperatures (°C): 139 (■), 138 (□), 137 (●), 136 (○), 135 (▲), 134 (△), 133 (×).

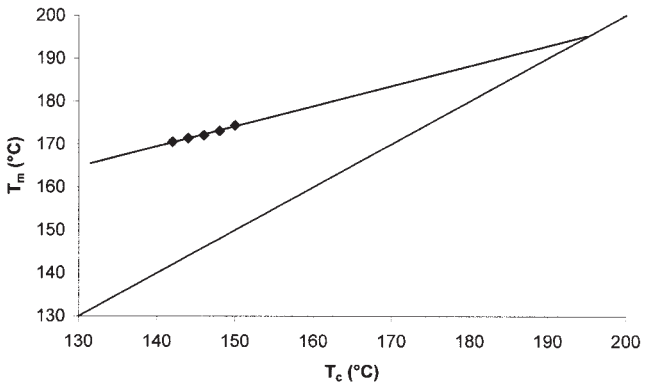

Figure 13 Hoffman–Weeks plot of apparent melting temperature versus crystallization temperature for determining the equilibrium melting temperature of *trans*-1,2-PPD.

where T_m^0 is the equilibrium melting temperature and γ is the ratio of the thickness of the grown crystallite to the thickness of the critical crystalline nucleus.[31] In Figure 13, the melting temperatures, registered at the maximum of the peak for the isothermally crystallized *trans*-1,2-PPD, are reported as a function of T_c. On the basis of eq. (14), the extrapolation of the straight line to the intersection with the $T_m = T_c$ line yielded the equilibrium melting temperature of 194°C.

CONCLUSIONS

Trans-1,2-syndiotactic polypentadiene was prepared at −30°C by using the catalyst system $CoCl_2(P^iPrPh_2)^2$–MAO. The polymer microstructure was attributed on the basis of NMR and FTIR analysis of the polymer.

An extensive study on the thermal behavior of *trans*-1,2-PPD was performed by DSC investigations. *Trans*-1,2-PPD crystallizes in a relatively short range of temperatures and its crystallization speed is generally fast as shown by the $t_{0.5}$ values obtained from isothermal crystallization curves, and by the t_{max} values calculated from the nonisothermal crystallization data. The attitude to a fast crystallization is well defined by the calculated CRC value of 122 h^{-1}. Very similar values of the activation energy of melt crystallization were calculated from isothermal and nonisothermal crystallization data. The applicability of several kinetics approaches for nonisothermal melt crystallization was examined. The Avrami analysis modified by Jeziorny exhibited two distinct crystallization regions with a transition when the fraction of crystallizable material reached a value of about 0.85. The Ozawa method failed to describe the nonisothermal melt crystallization process. The equilibrium melting temperature derived from the Hoffman–Weeks approach equaled 194°C.

Trans-1,2-syndiotactic polypentadiene and 1,2-syndiotactic polybutadiene are members of 1,2-polydienes family. The activation energy of melt crystallization ($\Delta E \sim -200$ kJ/mol) and the CRC value of 122 h^{-1} observed for *trans*-1,2-PPD are significantly lower than the ones obtained for 1,2-syndiotactic polybutadiene ($\Delta E = -509$ kJ/mol and CRC = 203 h^{-1}), respectively. These results indicate that the energy barrier overcome for melt crystallization of *trans*-1,2-PPD is smaller than that of 1,2-syndiotactic polybutadiene and that *trans*-1,2-PPD is a slower crystallizing system.

References

1. Ricci, G.; Italia, S.; Comitani, C.; Porri, L. Polymer Commun 1991, 32, 514.
2. Ricci, G.; Italia, S.; Giarrusso, A.; Porri, L. J Organomet Chem 1993, 451, 67.
3. Ricci, G.; Morganti, D.; Sommazzi, A.; Santi, R.; Masi, F. J Mol Catal A: Chem 2003, 204, 287.
4. Ricci, G.; Forni, A.; Boglia, A.; Sonzogni, M. Organometallics 2004, 23, 3727.
5. Ricci, G.; Forni, A.; Boglia, A.; Motta, T.; Zannoni, G.; Canetti, M.; Bertini, F. Macromolecules, 2005, 38, 1064.
6. Bertini, F.; Canetti, M.; Ricci, G. J Appl Polym Sci 2004, 92, 1680.
7. Bertini, F.; Canetti, M.; De Chirico, A.; Ricci, G. J Appl Polym Sci 2003, 88, 2737.
8. Ricci, G.; Motta, T.; Boglia, A.; Alberti, E.; Zetta, L.; Bertini, F.; Arosio P.; Meille S. V. Macromolecules, to appear.
9. Ciampelli, F.; Lachi, M. P.; Tacchi Venturi, M.; Porri, L. Eur Polym Mater 1967, 3, 353.
10. Beebe, D. H.; Gordon, C. E.; Thudium, R. N.; Thockmorton, M. C.; Hanlon, T. L. J Polym Sci 1978, 16, 2285.
11. Bovey, F. A. High Resolution NMR of Macromolecules; Academic Press: New York, 1972.
12. Avrami, M. J Chem Phys 1939, 7, 1103.
13. Avrami, M. J Chem Phys 1940, 8, 212.
14. Cebe, P.; Hong, S. D. Polymer 1986, 27, 1183.
15. Mandelkern, L. Crystallization of Polymers, Vol. 2; Academic Press: New York, 1977.
16. Kissinger, H. E. J Res Natl Bur Stand (US) 1956, 57, 217.
17. Khanna, P. Polym Eng Sci 1990, 30, 1615.
18. Di Lorenzo, M. L.; Silvestre, C. Prog Polym Sci 1999, 24, 917.
19. Jeziorny, A. Polymer 1978, 19, 1142.
20. Ziabicki, A. Colliod Polym Sci 1974, 252, 433.
21. Ziabicki, A. J Chem Phys 1968, 48, 4368.
22. Ziabicki, A. Appl Polym Sci 1967, 6, 1.
23. Kim, S. H.; Ahn, S. H.; Hirai, T. Polymer 2003, 44, 5625.
24. Ozawa, T. Polymer 1971, 12, 150.
25. Eder, M.; Wlochowicz, A. Polymer 1983, 24, 1593.
26. Addonizio, M. L.; Martuscelli, E.; Silvestre, C. Polymer 1987, 28, 183.
27. Cebe, P. Polym Comp 1988, 9, 271.
28. Liu, S.; Yu Y.; Zhang, H.; Mo, Z. J Appl Polym Sci 1998, 70, 2371.
29. Gan, Z.; Zhang, J.; Jiang, B. J Appl Polym Sci 1997, 63, 1793.
30. Hoffman, J. D.; Weeks, J. J. J Res Natl Bur Stand (US) 1962, 66, A13.
31. Alamo, R. G.; Viers, B. D.; Mandelkern, L. Macromolecules 1995, 28, 3205.